Original Article

Intratumor immune heterogeneity across simulated core biopsy sizes in non-small cell lung cancer: an exploratory study

Shaowen Lyu[1#], Kobe Reynders[1#], Iris E. W. G. Laven[1], Christel Faes[2], Birgit Weynand[3], Lisa M. Hillen[4], Paul De Leyn[5], Lizza E. L. Hendriks[6], Els Wauters[7], Maarten Lambrecht[8], Rianne D. W. Vaes[1], Dirk De Ruysscher[1]

[1]Department of Radiation Oncology (Maastro), GROW Research Institute for Oncology and Reproduction, Maastricht University Medical Center+, Maastricht, The Netherlands; [2]Data Science Institute, Center for Statistics Hasselt University, Hasselt, Belgium; [3]Department of Pathology, KU Leuven-University of Leuven, University Hospitals Leuven, Leuven, Belgium; [4]Department of Pathology, GROW Research Institute for Oncology and Reproduction, Maastricht University Medical Center+, Maastricht, The Netherlands; [5]Department of Thoracic Surgery, University Hospitals Leuven, Leuven, Belgium; [6]Department of Pulmonary Diseases, GROW Research Institute for Oncology and Reproduction, Maastricht University Medical Center+, Maastricht, The Netherlands; [7]Respiratory Oncology Unit (Pulmonology), University Hospitals Leuven, Leuven, Belgium; [8]Department of Radiation Oncology, University Hospitals Leuven, Leuven, Belgium

Contributions: (I) Conception and design: S Lyu, K Reynders, LEL Hendriks, E Wauters, M Lambrecht, D De Ruysscher; (II) Administrative support: S Lyu, K Reynders; (III) Provision of study materials or patients: B Weynand, P De Leyn, E Wauters, M Lambrecht; (IV) Collection and assembly of data: S Lyu, K Reynders, IEWG Laven, C Faes, B Weynand; (V) Data analysis and interpretation: S Lyu, K Reynders, IEWG Laven, C Faes, RDW Vaes, D De Ruysscher; (VI) Manuscript writing: All authors; (VII) Final approval of manuscript: All authors.

[#]These authors contributed equally to this work as co-first authors.

Correspondence to: Rianne D. W. Vaes, PhD. Department of Radiation Oncology (Maastro), GROW Research Institute for Oncology and Reproduction, Maastricht University Medical Center+, Dr Tanslaan 12, 6229 ET Maastricht, The Netherlands. Email: rianne.vaes@maastro.nl.

Background: Immune checkpoint blockade (ICB) is widely used to treat patients with non-small cell lung cancer (NSCLC). However, intratumor (immune) heterogeneity may significantly impact the therapeutic efficacy of ICBs. It remains unknown whether larger core biopsies better represent the intratumor heterogeneity. This study aimed to explore the intra- and interpatient heterogeneity of selected immune-related parameters on varying simulated biopsy core sizes.

Methods: In this exploratory prospective cohort study, patients with stage I–III NSCLC who had undergone curative-intent surgery, with or without neoadjuvant chemotherapy or chemoradiation, were enrolled. Intratumor immune heterogeneity was assessed using quadruple immunofluorescence stainings (CD31, Ki67, CD4, CD8, CD68, FOXP3, PD-L1, Pan-keratin, and DAPI) on resected tumor specimens. Digital images were used to simulate biopsy cores ranging from 1- to 4-mm in diameter. Heterogeneity was quantified using the quartile coefficient of dispersion (QCD) across 250 randomly selected subregions per core size.

Results: Tumor specimens from 29 patients were analyzed, including 10 patients who had received neoadjuvant therapy. Intratumor QCD values decreased significantly with increasing simulated biopsy core diameter for all markers. Nonetheless, substantial spatial heterogeneity persisted for programmed death-ligand 1 (PD-L1), with 58.8% of patients showing heterogeneous distribution, even in 4-mm simulated biopsy cores.

Conclusions: Larger biopsy core sizes were associated with reduced intratumor heterogeneity for most immune markers, suggesting a better reflection of the tumor immune landscape of the whole tumor. However, PD-L1 expression remained spatially heterogeneous even in larger cores. Further validation in larger prospective cohort studies will be essential to determine the translational relevance of heterogeneity metrics and to better inform biopsy sampling strategies in routine clinical practice.

Keywords: Non-small cell lung cancer (NSCLC); biopsy; intratumor immune heterogeneity; programmed death-ligand 1 (PD-L1)

© AME Publishing Company.

Submitted Jan 05, 2026. Accepted for publication May 24, 2026. Published online Jun 26, 2026.
doi: 10.21037/tlcr-2026-1-0017
View this article at: https://dx.doi.org/10.21037/tlcr-2026-1-0017

Introduction

Immune checkpoint blockade (ICB) has been widely implemented in the curative and palliative treatment setting for patients with non-small cell lung cancer (NSCLC) (1-8). Besides tumor stage and patient characteristics, the selection of patients to receive ICB is predominantly based on the expression of programmed death-ligand 1 (PD-L1) on tumor cells (9). Although ICB leads to long-lasting remissions or cure in a subset of patients, a considerable number of patients do not have a disease response (primary resistance) or develop resistance after obtaining an initial clinical or radiological response (acquired resistance), despite the presence of PD-L1 (10-14). Conversely, also a subgroup of patients without PD-L1 expression on the tumor have been shown to respond to PD-(L)1 inhibition (15). This has prompted clinicians to investigate the underlying causes of ICB resistance, with intratumor heterogeneity emerging as a significant contributing factor (16-18).

Intratumor heterogeneity, which mainly denotes the genetic, epigenetic, and microenvironmental differences within different regions in a single tumor, has widely been shown to have vital implications in treatment outcomes (19-22). However, the intratumor immune heterogeneity, which includes the presence and distribution of immune cells in the tumor microenvironment (TME), is often overlooked despite their important functional roles. In the TME, immune cells can either suppress tumor formation or promote tumorigenesis. It has recently been shown that the extent of immune cell infiltration differed within and across lung tumors. Whereas T-helper cells and M2 macrophages were consistently present across all tumor regions, cytotoxic T-cells showed more regional variations (23). Also, it is suggested that the expression level of PD-L1 on tumor cells is heterogeneously distributed across a single tumor mass (24,25). As a consequence, a single tumor biopsy, by definition taken from one region only, may underestimate the immunological landscape of the whole tumor.

For patients with lung cancer, core needle biopsy or endobronchial ultrasound (EBUS)/endoscopic ultrasound (EUS)-guided transbronchial needle aspiration (EBUS/EUS-TBNA) are the most often used biopsy procedures because of its minimally invasive nature and relatively high diagnostic yield (26). Biopsies from the primary tumor or lymph nodes are usually obtained with needles ranging in size from 19 to 25 gauge, resulting in biopsies with a core diameter of 1 to 4 mm (27). However, it remains unknown how representative these biopsies are for the whole tumor in terms of the intratumor immune heterogeneity. Obtaining more or larger biopsy specimens is generally conceived to be better, however, in clinical practice this is not always feasible as it may come with an increased risk of complications (28).

Highlight box

Key findings

- Using a computational simulation-based approach, intra- and interpatient heterogeneity of different immune parameters in tumor resection material from patients with non-small cell lung cancer was quantified using the quartile coefficient of dispersion. Increasing simulated biopsy core size was associated with reduced intratumor immune heterogeneity, suggesting improved sampling representativeness. However, programmed death-ligand 1 (PD-L1) expression remained spatially heterogeneous even in large biopsy cores. Differences in $FOXP3^+$ cell heterogeneity were observed between tumor stage and treatment groups, however, no causal relationship could be established.

What is known and what is new?

- Intratumor heterogeneity is increasingly recognized as a key factor influencing biomarker assessment and response to immune checkpoint blockade. However, the extent to which biopsy core size affects the representativeness of this heterogeneity remains unclear.
- This study presents the results of a quantitative analysis of immune heterogeneity across simulated biopsy core sizes and demonstrates that the sampling size influences the heterogeneity of most immune markers. Importantly, this study showed persistent spatial variability of PD-L1, even in larger biopsy core diameters.

What is the implication, and what should change now?

- These findings highlight the challenges of assessing spatially heterogeneous biomarkers using limited biopsy material and suggest that sampling strategies may influence observed heterogeneity patterns. Although this study is exploratory and simulation-based, it provides a conceptual framework for future research. Validation in larger prospective cohorts will be essential to determine the translational relevance of heterogeneity metrics and to better inform biopsy sampling strategies in routine clinical practice.

© AME Publishing Company.

Yet, there is no clear consensus on the optimal biopsy core size or its adequacy in representing the whole tumor in terms of intratumor immune heterogeneity (25). In this exploratory cohort study, we assessed both intra- and interpatient heterogeneity of selected immune parameters using simulated biopsy cores derived from tumor resection specimens of patients with NSCLC. We used a computational approach to calculate the quartile coefficient of dispersion (QCD) as metric for intratumor immune heterogeneity and interpatient heterogeneity. These findings may provide valuable insights into intratumor immune heterogeneity and contribute to the design of future large prospective cohort studies. We present this article in accordance with the STROBE reporting checklist (available at https://tlcr.amegroups.com/article/view/10.21037/tlcr-2026-1-0017/rc).

Methods

Study design and patients

In this exploratory prospective cohort study, patients diagnosed with stage I–III NSCLC who received curative intent (bi)lobectomy or pneumonectomy with or without neoadjuvant chemotherapy (CTx) or chemoradiation (CRT) were enrolled at the University Hospitals Leuven (UZ Leuven, Leuven, Belgium) between September 2014 and December 2016. Patients were selected through the multidisciplinary oncology consultation for lung cancer. Standard-of-care treatment was not altered for study participation. Key exclusion criteria included the use of immunosuppressive medication (i.e., active long-term corticosteroid use, the use of NSAIDs taken until 5 days before surgery), active autoimmune diseases, maximum tumor diameter of 2 cm or less, and tumors with a cavitation on computed tomography (CT) scan. This study was conducted in accordance with the Declaration of Helsinki and its subsequent amendments. The study was approved by the Medical Ethics Committee of UZ/KU Leuven (S56031). All patients included in the study have provided written informed consent.

Clinical data collection

The following patient characteristics were collected: sex, age, smoking status, histology, maximum tumor diameter on preoperative CT scan, histology, pathological tumor stage (staging recoded to TNM8 for all patients), PD-L1 tumor proportion score (TPS), type of surgery, and type of induction treatment if applicable.

Tissue collection and handling

Resection specimens were immediately transferred to the department of Pathology (University Hospitals Leuven, Leuven, Belgium), where a cross-section of 5-mm thickness was taken with a maximum diameter of 5-cm. If the tumor was larger than 5-cm, a random cross-section was taken up to 5-cm in diameter. This cross-section was divided into two separate slices, one was stored as formalin-fixed paraffin embedded (FFPE) and the other one was fresh frozen stored at –80 ℃ for future analyses. From the FFPE block, 25 serial sections of 5-µm thickness were made for immunofluorescence staining.

Immunofluorescence staining

For each patient, 9 different parameters of interest were stained in 6 (quadruple) immunofluorescence staining combinations. These markers included CD31, Ki67, CD4, CD8, CD68, FOXP3, PD-L1, Pan-keratin, and 4',6'-diamidino-2-phenylindole (DAPI). $CD31^+$ cells represent vascular endothelial cells, Ki67 is a well-known indicator of proliferation, and $CD4^+$ and $CD8^+$ cells represent T-helper and cytotoxic T-cells, respectively. $CD68^+$ cells represent macrophages, and $FOXP3^+$ represent T_{reg}-cells. PD-L1 was stained because anti-PD-L1 blockade therapy is the primary ICB. However, PD-L1 expression was assessed using a research-grade antibody as part of the multiplex immunofluorescence panel. Accordingly, PD-L1 analyses focused on spatial heterogeneity rather than absolute clinical scoring (i.e., PD-L1 TPS categories). Pan-keratin was included to assess the localization of tumor cells. Finally, nuclei were counterstained with DAPI. A detailed description of the immunofluorescence staining procedures is included in Appendix 1. Technical details of the antibodies used and the immunofluorescence staining combinations are represented in Tables S1,S2.

Immunofluorescence imaging and data extraction

Stained slides were mounted on a Zeiss Axioscanner 7. Using the Zen Lite Imaging Software, a region of interest (ROI) was manually defined for each sample. This ROI consisted of the whole tumoral tissue, while excluding empty regions, adjacent normal lung tissue, and regions

© AME Publishing Company.

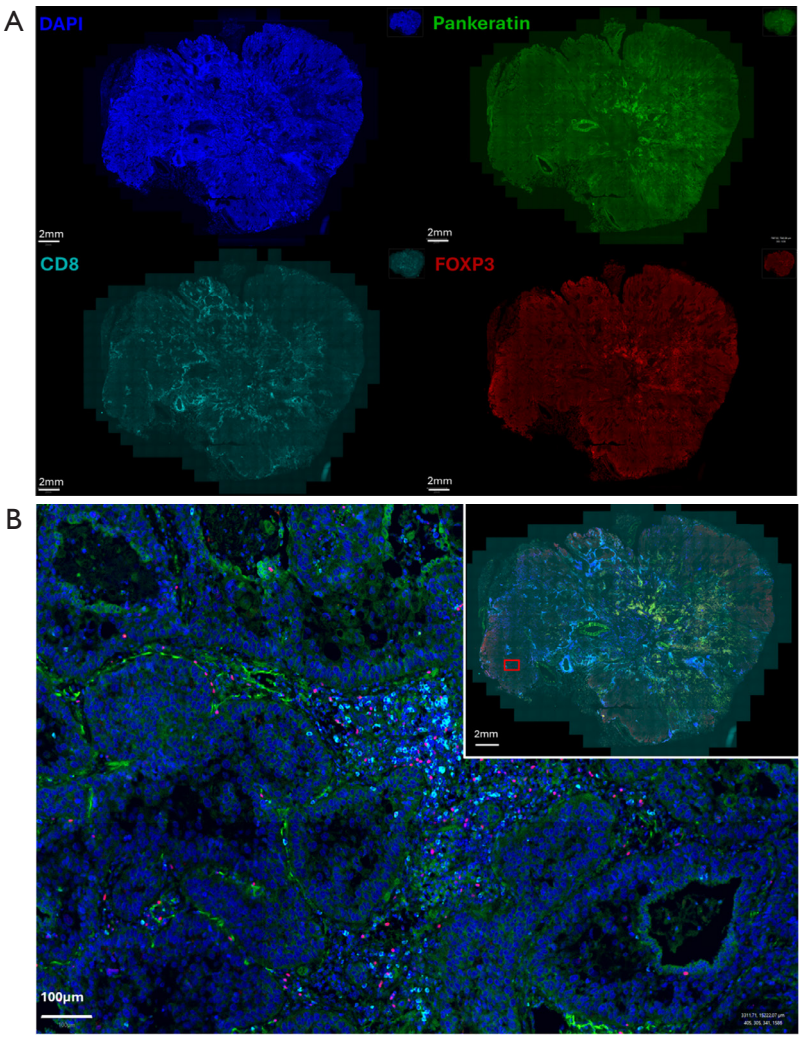

Figure 1 Quadruple immunofluorescent staining. (A) Representative images of each individual staining, including DAPI, Pan-keratin, CD8, and FOXP3. (B) The merged image of these individual immunofluorescent stainings.

with 'abnormal' tissues (Figure S1). Next, each sample was scanned for immunofluorescent signal using 4 wavelengths (Table S2), covering every mentioned parameter of interest including DAPI (*Figure 1*). Digital images were uploaded into QuPath imaging software (v.0.1.2) (29). For each staining parameter, manual cell detection was done by defining settings for minimal detection threshold, minimum and maximum possible cell area, background staining threshold to reduce background noise and sigma value to stop nuclei fragmentation. Using the automatic cell detection function, centroid coordinates (X,Y) for every individual cell in a representative ROI were determined. This process is represented in Figure S2. The threshold-based cell detection parameters were defined per tumor sample and then applied uniformly to the entire tumor region, such that no variability in detection settings occurred across ROIs within a given tumor. Consensus on thresholds was reached when there was >95% concordance between the manual scoring and the automated output. Selection of these thresholds was done in close collaboration with an experienced thoracic pathologist.

Intratumor and interpatient immune heterogeneity metric

Tumor heterogeneity was quantified using the QCD (30), a measure of spread with 0% showing no variation and 100% large amount of variation, for both density (QCD_D) and incidence (QCD_I) of different cell types. Cell density

© AME Publishing Company.

was defined as the number of cells per area size, whereas the incidence was defined as the number of cells of a certain type divided by all DAPI cells. The QCD was measured within a patient (intratumor QCD) and between patients (interpatient QCD). To calculate the QCD, subregions were randomly selected digital discs from the patient's tumor sample with varying simulated biopsy core diameters (1-, 2-, 3-, and 4-mm). For each patient, 250 randomly selected digital discs were selected for each simulated core biopsy diameter size. Details regarding calculation of the QCD are described in Appendix 1. The overall density (QCD_D) or incidence (QCD_I) was obtained from the median value of the taken samples for each patient. In the absence of validated biological or clinical QCD thresholds, heterogeneity was analyzed on a continuous scale. For exploratory descriptive purposes, an arbitrary QCD cut-off of ≤0.25 (first quartile), was initially explored, and robustness was assessed using sensitivity analysis with two alternative arbitrary thresholds (QCD ≤0.20 and ≤0.30) (Tables S3,S4). All simulations of randomly selection digital discs and calculations of density and incidence were conducted in R software (Version 3.4.0; R Foundation for Statistical Computing, Vienna, Austria).

Statistical analyses

Patient data and outcome parameters were analyzed and visualized using both IBM SPSS Statistics for Microsoft Windows (Version 29.0.2.0, IBM Corp.) and GraphPad Prism (Version 11.0.0; GraphPad Software, LLC). QCD values are reported as median and interquartile range (IQR). Differences in intratumor QCD across simulated biopsy diameter groups were assessed using the non-parametric Friedman test, followed by post-hoc pairwise comparison using Dunns' multiple comparison test with correction for multiple testing. Only patients with QCD values available for all four diameter groups were included as this statistical test requires complete repeated-measures data. No imputation of missing values was performed. Comparisons between two independent groups were performed using the Mann-Whitney *U* test. In case of more than two groups, the Kruskal-Wallis test with Bonferroni correction for multiple testing was used. Statistical significance was defined as a P value of less than 0.05. Interpatient QCD values are presented descriptively to illustrate cohort-level patterns of between-patient heterogeneity. Formal statistical comparisons were not performed because interpatient QCD represents a single aggregate measure per marker and diameter.

Results

Patient characteristics

A total of 50 patients were enrolled in this exploratory cohort study. From these patients, 21 patients were excluded because no tumor tissue was present (n=3), no sample could be collected because of potential interference with routine diagnostic evaluation (n=3), no tumor could be collected due to invasion in the chest wall (n=1), poor tissue quality or non-NSCLC histology (n=5), or due to practical limitations related to tissue handling, including receiving tumor resection material outside working hours (n=7), and cases where resection material had already been formalin-fixed before tissue processing could be initiated (n=2). As such, tumor tissue material was analyzed from a total of 29 patients. Patient characteristics are presented in *Table 1*. Mean age at the time of surgery was 66.5±10.0 years and 68.9% were male. Mean tumor size (largest diameter on the macroscopic pathology report) was 43.8±18.1 mm. Nineteen patients received surgery alone, whereas 10 patients received neoadjuvant therapy prior to surgery. Of these patients, 6 patients (20.7%) received neoadjuvant CTx and 4 patients (13.8%) neoadjuvant CRT (Table S5). Neoadjuvant CTx consisted of a cisplatin-based regimen in combination with either pemetrexed or gemcitabine. Preoperative concurrent CRT consisted of radiotherapy (46 Gy/23 fractions) combined with 2 cycles of cisplatin-etoposide. Furthermore, 10 patients (34.5%) of the 29 included patients were diagnosed with stage I disease, 9 patients (31.0%) with stage II, and 10 patients with stage III (34.5%).

Intratumor immune heterogeneity of all patients

The intratumor immune heterogeneity of all patients were visualized using violin plots of both QCD_D and QCD_I for $CD31^+$, $Ki67^+$, $CD4^+$, $CD8^+$, $CD68^+$, $FOXP3^+$, and $PD\text{-}L1^+$ in *Figure 2A* and *Figure 2B*, respectively. Overall, the median QCD_I of all markers are lower compared to the median QCD_D, except for $FOXP3^+$ (*Figure 2A,2B*). These results indicate that the number of positive cells for a specific marker, divided by the total number of all DAPI-positively stained cells in that area, were less affected by variations in different tissue composition in the sub-regions. Each marker showed significant differences in heterogeneity

© AME Publishing Company.

Table 1 Baseline characteristics

Variable	Overall (N=29)	Upfront surgery cohort (N=19)	Neoadjuvant therapy cohort (N=10)
Sex (male)	20 (69.0)	12 (69.2)	8 (50.0)
Age (years)	66.5±10.0	68.6±8.7	62.4±10.5
Active smoker	14 (48.2)	12 (63.2)	2 (20.0)
Pack years (years)	35.7±14.9	33.7±15.5	41±9.9
Tumor diameter (mm)	43.8±18.1	42.2±18.1	47.0±17.7
Induction therapy			
No induction therapy	19 (65.5)	19 (100.0)	0 (0.0)
Chemotherapy	6 (20.7)	0	6 (60.0)
Chemoradiation	4 (13.8)	0	4 (40.0)
Type of surgery			
Lobectomy	19 (65.5)	12 (63.1)	7 (70.0)
Pneumonectomy	6 (20.7)	4 (21.1)	2 (20.0)
Sleeve lobectomy	4 (13.8)	3 (15.8)	1 (10.0)
Histology			
Adenocarcinoma	12 (41.4)	7 (36.8)	5 (50.0)
Squamous carcinoma	14 (48.3)	11 (57.9)	3 (30.0)
Large cell carcinoma	2 (6.9)	1 (5.3)	1 (10.0)
Pathological tumor stage			
Stage I	10 (34.5)	9 (47.4)	1 (10.0)
Stage II	9 (31.0)	4 (21.1)	5 (50.0)
Stage III	10 (34.5)	6 (31.6)	4 (40.0)
PD-L1 TPS			
<5%	13 (44.8)	8 (42.1)	5 (50.0)
≥5% and <50%	14 (48.3)	9 (47.7)	5 (50.0)
≥50%	2 (6.9)	2 (10.5)	0

Data are presented as mean ± standard deviation or n (%). PD-L1, programmed death-ligand 1; TPS, tumor proportion score.

between the simulated biopsy core diameter groups. The QCD_I of all markers in the 1- and 2-mm diameter groups were significantly higher than in the 4 mm diameter group [1- *vs.* 4-mm: $CD31^+$: median 0.352 (IQR, 0.217–0.587) *vs.* 0.224 (0.087–0.389), P<0.001; $Ki67^+$: median 0.274 (IQR, 0.163–0.514) *vs.* 0.166 (0.093–0.350), P<0.001; $CD4^+$: median 0.371 (IQR, 0.257–0.667) *vs.* 0.197 (0.136–0.465), P<0.001; $CD8^+$: median 0.369 (IQR, 0.263–0.763) *vs.* 0.137 (0.073–0.366), P<0.001; $CD68^+$: median 0.243 (IQR, 0.168–0.335) *vs.* 0.128 (0.098–0.192), P<0.001; $FOXP3^+$: median 0.448 (IQR, 0.354–0.645) *vs.* 0.249 (0.179–0.360), P<0.001; $PD\text{-}L1^+$: median 0.429 (IQR, 0.310–0.587) *vs.* 0.287 (0.171–0.366), P<0.001] (*Figure 2A*,*2B*). In the 3-mm diameter group, only the QCD_I of $CD31^+$ [median 0.240 (0.101–0.449) *vs.* 0.224 (0.087–0.389), P=0.02] and $PD\text{-}L1^+$ [0.321 (0.188–0.390) *vs.* 0.287 (0.171–0.366), P=0.01] were significantly higher compared to the 4-mm group. Notably, $CD68^+$ showed the lowest intratumor QCD_I across all diameters.

Table 2 report the percentage of patients below the threshold of the arbitrary cut-off of ≤0.25. Overall, an increased diameter of the analyzed sub-region resulted in an

© AME Publishing Company.

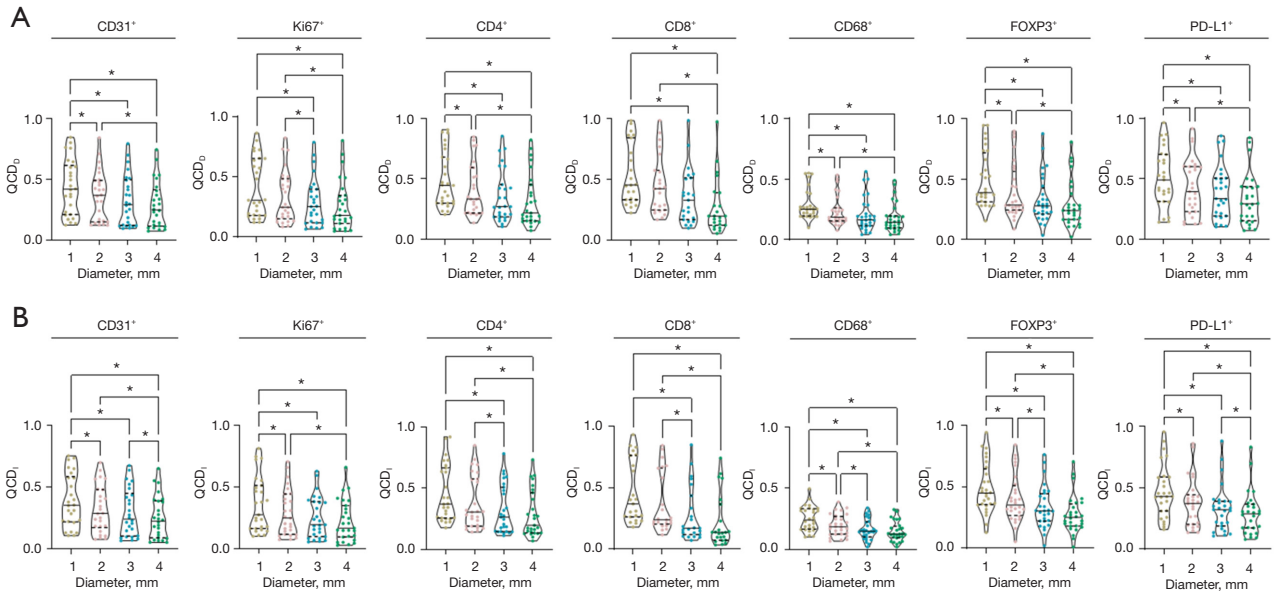

Figure 2 The intratumor immune heterogeneity in all patients. (A) Violin plots of the QCD_D, representing the number of positively stained cells of each marker per area size. (B) Violin plots of the QCD_I, representing the number of positively stained cells of each marker divided by the total number of cells ($DAPI^+$) per area. Violin plots show the distribution of QCD values, horizontal lines indicate the median and interquartile range. Only patients with QCD values available for all four diameters were included (complete repeated-measures data); $CD31^+$ (n=26), $Ki67^+$ (n=27), $CD4^+$ (n=27), $CD8^+$ (n=23), $CD68^+$ (n=28), $FOXP3^+$ (n=28), $PD\text{-}L1^+$ (n=27). Differences in intratumor heterogeneity across simulated biopsy diameters have been assessed using the Friedman test, followed by post-hoc Dunn's multiple comparisons test. *, P<0.05. PD-L1, programmed death-ligand 1; QCD, quartile coefficient of dispersion; QCD_D, QCD density; QCD_I, QCD incidence.

Table 2 Percentage of patients with a QCD below the arbitrary threshold of ≤0.25

Marker	QCD_I ≤0.25 (%)				QCD_D ≤0.25 (%)			
	1 mm	2 mm	3 mm	4 mm	1 mm	2 mm	3 mm	4 mm
$CD31^+$	39.3	46.4	51.9	57.7	35.7	42.9	44.4	50.0
$Ki67^+$	48.3	55.2	60.7	63.0	37.9	55.2	50.0	59.3
$CD4^+$	24.1	34.5	50.0	51.9	13.8	34.5	42.9	55.6
$CD8^+$	31.0	60.7	66.7	73.9	13.8	35.7	45.8	65.2
$CD68^+$	51.7	72.4	78.6	82.1	51.7	72.4	75.0	78.6
$FOXP3^+$	6.9	20.7	35.7	50.0	3.4	31.0	42.9	57.1
$PD\text{-}L1^+$	17.2	31.0	39.3	40.7	13.8	27.6	35.7	37.0

PD-L1, programmed death-ligand 1; QCD, quartile coefficient of dispersion; QCD_D, QCD density; QCD_I, QCD incidence.

increased percentage of patients that meet this criterion. For $CD8^+$, $CD68^+$, and $Ki67^+$, more than 60% of the patients have a QCD_I ≤0.25 in the 3- and 4-mm diameter group. For $FOXP3^+$ and $PD\text{-}L1^+$, 50.0% or less of the patients have a QCD_I ≤0.25 in the 3- and 4-mm diameter group. Strikingly, for $PD\text{-}L1^+$, only 40.7% of patients have a QCD_I ≤0.25 in the 4-mm group, which is the lowest percentage among all other markers. Sensitivity analyses using alternative QCD_I thresholds (≤0.20 and ≤0.30) showed consistent patterns across biopsy diameters compared to QCD_I ≤0.25, with increasing core size associated with a higher proportion of patients below all thresholds, while PD-L1 heterogeneity

© AME Publishing Company.

remained comparatively high, even in larger cores (Tables S3,S4). For QCD_D, the percentages of patients below the arbitrary cut-off of ≤0.25 were lower compared to the QCD_I numbers, except for $FOXP3^+$ showing higher percentages for the 2, 3 and 4 mm group.

Additional exploratory analyses were performed to assess differences in intratumor heterogeneity across clinical and pathological variables (Tables S6-S12). Significant differences were observed only for $FOXP3^+$ cells in relation to tumor stage and induction therapy. Specifically, QCD_I values were significantly higher in patients with stage II disease compared to stage I across all biopsy core diameters [1-mm: 0.358 (0.267–0.969) *vs.* 0.542 (0.463–0.780), adj. P=0.02; 2-mm: 0.249 (0.196–0.350) *vs.* 0.449 (0.380–0.656), adj. P=0.02; 3-mm: 0.187 (0.128–0.286) *vs.* 0.405 (0.290–0.492), adj. P=0.02; 4-mm: 0.170 (0.089–0.245) *vs.* 0.291 (0.235–0.395), adj P=0.03]. Similarly, QCD_I values for $FOXP3^+$ cells were higher in patients who received induction therapy compared to patients who received upfront surgery [1-mm: 0.566 (0.423–0.819) *vs.* 0.387 (0.315–0.539), P=0.04; 2-mm: 0.465 (0.367–0.737) *vs.* 0.317 (0.234–0.401), P=0.009; 3-mm: 0.426 (0.302–0.644) *vs.* 0.256 (0.177–0.315), P=0.005; 4-mm: 0.311 (0.247–0.579) *vs.* 0.204 (0.155–0.275), P=0.01].

Intratumor heterogeneity stratified by treatment

Following stratification by treatment, intratumor heterogeneity quantified by QCD_I and QCD_D was evaluated and compared between the 'upfront surgery' cohort and 'neoadjuvant therapy (CTx and CRT only)' cohort, as shown in *Figure 3* and Figure S3, respectively. Overall, no differences were observed between both groups, except for the QCD_I of $FOXP3^+$. The QCD_I remained overall higher in the tumor specimens of the neoadjuvant therapy cohort [1-mm: median 0.387 (IQR, 0.315–0.539) *vs.* 0.566 (0.423–0.819), P=0.04; 2-mm: median 0.317 (IQR, 0.234–0.401) *vs.* 0.465 (0.367–0.737), P=0.009; 3-mm: median 0.256 (IQR, 0.177–0.315) *vs.* 0.426 (0.302–0.644), P=0.005; and 4-mm: median 0.204 (IQR, 0.155–0.275) *vs.* 0.311 (0.248–0.579), P=0.01]. No significant differences between both cohorts were found in the QCD_D for $FOXP3^+$ (Figure S3). Because the neoadjuvant group comprised 6 patients treated with CTx and 4 patients with CRT, an exploratory statistical comparison between these two subgroups was performed (Figure S4). Overall, no significant differences in intratumor heterogeneity was observed, except for $CD68^+$, for which the QCD_I was significantly higher in patients treated with CRT compared to those treated with CTx.

Interpatient tumor immune heterogeneity

To assess variability in immune marker distribution across patients, interpatient heterogeneity was assessed using QCD_I values across the different simulated biopsy core diameters. The interpatient QCD_I values remain similar for all markers across the different diameter groups for all patients, but shows notable differences between the upfront surgery cohort and the neoadjuvant therapy cohort (*Figure 4A*,*4B*). Patients in the neoadjuvant therapy cohort show higher QCD_I values compared to the upfront surgery cohort for $CD4^+$ (4-mm diameter: 0.54 *vs.* 0.17), $CD8^+$ (4-mm diameter: 0.58 *vs.* 0.34), and $Ki67^+$ (4-mm diameter: 0.40 *vs.* 0.23). In contrast, the QCD_I values of $CD68^+$ (4-mm diameter: 0.09 *vs.* 0.24), $FOXP3^+$ (4-mm diameter: 0.18 *vs.* 0.53), and $PD\text{-}L1^+$ (4-mm diameter: 0.50 *vs.* 0.62) are lower in the neoadjuvant therapy cohort.

Discussion

A practical question in clinical practice is how representative a single biopsy of a particular diameter is for the intratumor immune heterogeneity of the whole tumor. By using a computational approach, the level of intratumor heterogeneity was assessed within an individual tumor and between patients for simulated core biopsy sizes varying between 1 and 4 mm. Our results demonstrated that increasing the diameter of each sub-region to 3- to 4-mm significantly reduced the QCD for all markers, suggesting less intratumor heterogeneity and a better representation of the immunological landscape within different sub-regions. Although median intratumor heterogeneity levels for most immune markers decreased with increasing biopsy core diameter and were overall low in the 4-mm simulated cores, PD-L1 expression remained spatially heterogeneous, even in larger biopsy cores. These data suggest that a single biopsy core of 4-mm may still provide incomplete representation of PD-L1 distribution within the tumor. Furthermore, intratumor heterogeneity of $FOXP3^+$ cells differed between treatment-naïve and post-neoadjuvant specimens, however, in the absence of matched pre-treatment samples, it remain speculative what causes these differences (i.e., baseline biological variability or therapy-related tissue remodeling). Finally, interpatient heterogeneity appeared largely independent of biopsy core size, indicating that variability between patients is driven

© AME Publishing Company.

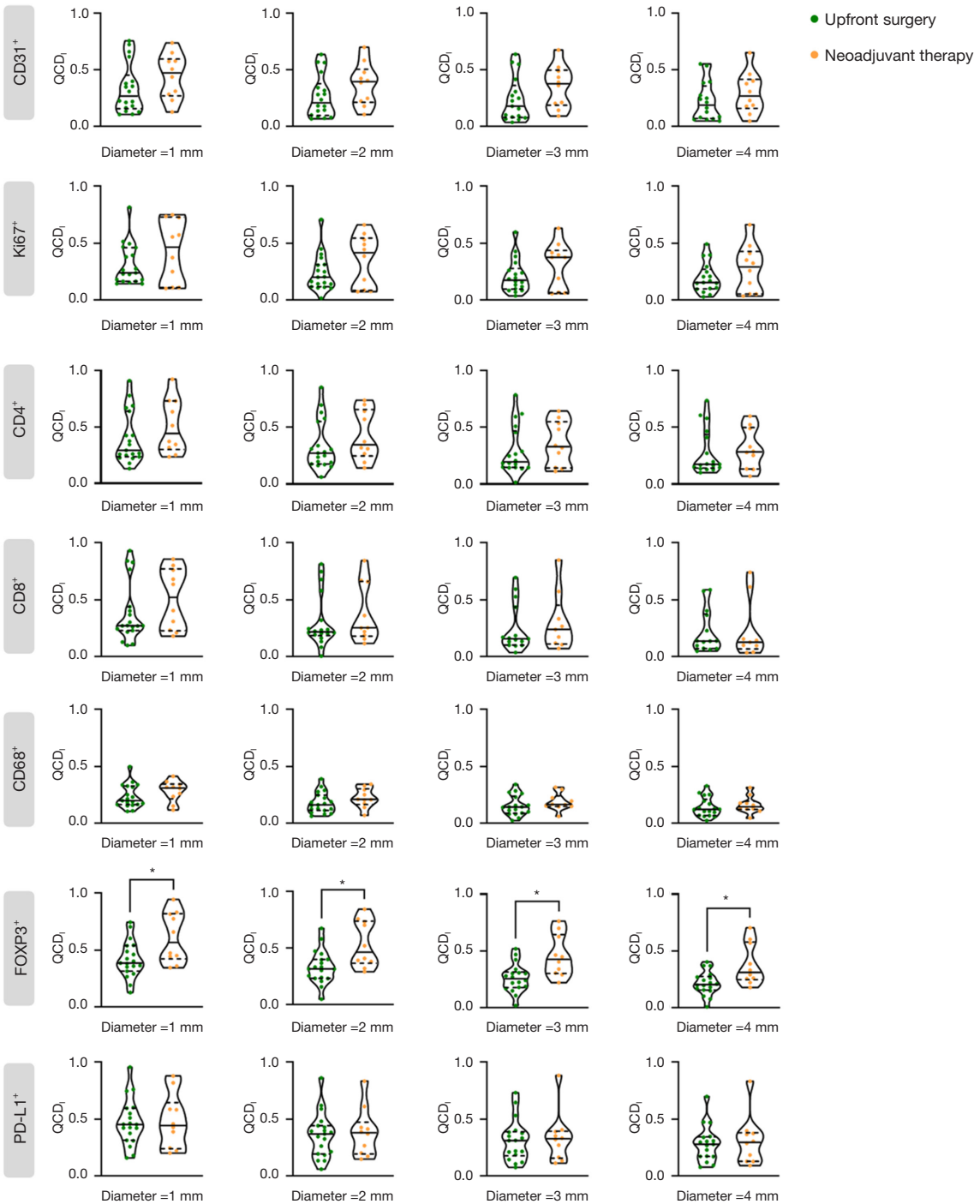

Figure 3 Intratumor immune heterogeneity (QCD_I) in the upfront surgery and neoadjuvant therapy cohort. Violin plots of the QCD_I, representing the number of positively stained cells of each marker divided by the total number of cells ($DAPI^+$) per area, for $CD31^+$, $Ki67^+$, $CD4^+$, $CD8^+$, $CD68^+$, $FOXP3^+$, and $PD\text{-}L1^+$ in each diameter group. Violin plots show the distribution of QCD_I values, horizontal lines indicate the median and interquartile range. Differences in QCD_I between the 'upfront surgery' cohort (n=19) and the 'neoadjuvant therapy' cohort (n=10) have been assessed using the Mann-Whitney *U* test. *, P<0.05. PD-L1, programmed death-ligand 1; QCD, quartile coefficient of dispersion; QCD_I, QCD incidence.

© AME Publishing Company.

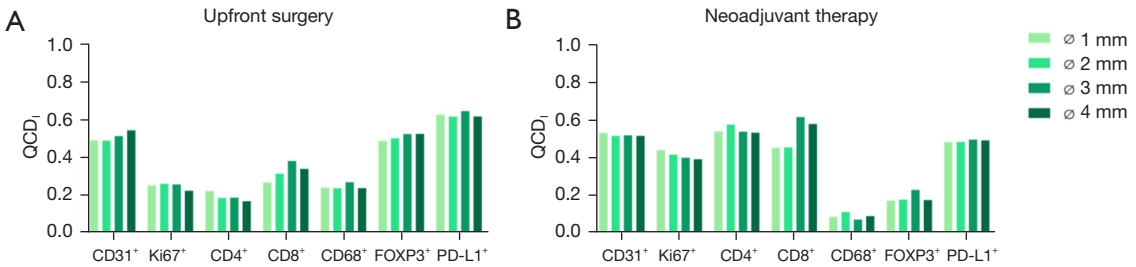

Figure 4 Interpatient tumor immune heterogeneity. The interpatient QCD_I in patients who underwent upfront surgery (A) and in patients who received neoadjuvant therapy (B), followed by surgical removal of the specimen. PD-L1, programmed death-ligand 1; QCD, quartile coefficient of dispersion; QCD_I, QCD incidence.

primarily by underlying biological differences rather than sampling procedures.

Our exploratory study assessed the intratumor heterogeneity of several immune parameters which could play a pivotal role in the prediction of immunotherapy response. We showed that the QCD_I of CD4$^+$, CD8$^+$, CD68$^+$, and FOXP3$^+$ cells gradually decreased when increasing the diameter of the subregions from 1- to 4-mm. Amongst all immune markers, CD68$^+$ showed the lowest heterogeneity, though, the clinical significance thereof remains questionable. A recent meta-analysis from Mei *et al.* showed that although the density of total CD68$^+$ tumor associated macrophages (TAMs) is not associated with overall survival, the localization and functional phenotype of these TAMs are potential prognostic predictors (31). Interestingly, we observed that the QCD_I of CD68$^+$ was significantly higher in patients treated with neoadjuvant CRT compared to those treated with neoadjuvant CTx only. Although radiation therapy can result in the influx of TAMs into the TME (32,33), in the absence of matched pre-treatment biopsy material, no causal relationship can be established, and the observed differences may only reflect baseline biological variation.

Here, we showed that PD-L1$^+$ cells remained heterogeneously distributed across simulated biopsy regions, even when larger biopsy core sizes were evaluated. These findings suggest that a single biopsy may capture only a localized representation of PD-L1 expression, potentially misrepresenting the overall tumor landscape. Also, this may be one of the underlying causes why a subset of patients with a high PD-L1$^+$ TPS fail to benefit from immunotherapy, while others with low or negative PD-L1 expression still derive clinical benefit (15). Importantly, the distribution of PD-L1$^+$ cells in this study was assessed using a research-grade antibody as part of the multiplex immunofluorescence panel, and therefore cannot be directly compared with clinically validated PD-L1 TPS assays. As such, the results should not be interpreted in terms of clinical decisions thresholds, but rather provide a conceptual understanding of spatial variability in PD-L1 distribution. Nevertheless, to date, only a limited number of studies have evaluated the reliability of core biopsy specimens for PD-L1 assessment. Most of these studies have primarily focused on tissue adequacy for PD-L1 testing, rather than on quantifying intratumor heterogeneity itself, and rarely consider the impact of biopsy core size (34,35). For example, Gompelmann *et al.* studied the correlation of PD-L1$^+$ tumor cells between EBUS-TBNA biopsies and surgical specimens and showed a high concordance rate with low specificity (36). Nevertheless, no significant correlation of the PD-L1 status between surgically resected specimens and cytology specimens was reported. Sun *et al.* showed heterogeneity between different needle core biopsies (diameter around 10 mm) within one tumor in 56% of the PD-L1 positive patients (37). This is comparable to the lower end of the PD-L1 heterogeneity range observed in our study, ranging from 90% for 1-mm to 59% for 4-mm cores. These findings suggest that larger biopsy cores, or alternatively, multiple smaller cores, may improve the representativeness of PD-L1 expression.

Although intratumor QCD values decreased with increasing core diameter, no comparable effect was observed for interpatient QCD values. This finding reflects the fact that interpatient variability is driven by biological differences between patients rather than sampling effects within a single tumor. In addition, differences in interpatient QCD values between both cohorts suggest that neoadjuvant therapy may differentially modulate heterogeneity across markers. It suggests that a more generalized patient response is shown following neoadjuvant therapy in

© AME Publishing Company.

immunoregulatory markers such as CD68$^+$, FOXP3$^+$, and PD-L1$^+$, while immune activation and proliferation (CD4$^+$, CD8$^+$, Ki67$^+$) is more variable between patients. Together, these findings suggest that neoadjuvant therapy may reduce interpatient variability in certain immunoregulatory markers while enhancing heterogeneity in markers of immune activation and tumor cell proliferation.

Tumor heterogeneity can be quantified using various metrics, including the coefficient of variation, which has been applied to assess spatial immune heterogeneity in previous studies (30,38). We used QCD because of its robustness, as it captures the relative dispersion based on interquartile ranges. This makes the metric less sensitive to outliers and independent of the mean value, unlike the coefficient of variation, which can be skewed by extreme values and low mean counts. Our study results support the utility of QCD in this context, since we observed the gradual decrease of the QCD_I with increasing subregion size independent of the relative abundance of these markers. Notably, patients with widely varying number of positively stained cells still exhibit similar QCD_I values (Figure S5). This suggests that QCD_I effectively captures the spatial distribution patterns of immune cells rather than their absolute counts, highlighting its value as a heterogeneity metric that is not confounded by cell density alone. However, it should be noted that the metric does not provide information on the number of immune cells within the tumor.

This study has several limitations. First, the relatively small and heterogeneous cohort limits statistical power and precludes robust subgroup analyses. Also, our dataset suffered from missing data (Table S13). In particular for repeated-measure analyses, only complete cases could be included, resulting in further reduction the effective sample size and limiting statistical power. Accordingly, this study should be interpreted as exploratory, with the primary aim to assess which biopsy core diameter is theoretically required to adequately capture intratumor immune heterogeneity within an individual tumor and providing a conceptual framework for future studies. Second, the study is based on a simulation approach using 2D biopsy regions extracted from resection specimens, which do not fully recapitulate real-world biopsy procedures such as EBUS/EUS-TBNA or CT-guided biopsies or the inherent 3D tissue architecture. Nevertheless, the 2D simulation approach aligns with the current clinical pathology workflow; clinical decisions are currently made based on routine pathological assessment, including PD-L1 TPS, on 2D histological sections. Future validation studies using matched diagnostic biopsy specimens and corresponding resection material will be essential to assess real-world applicability. Third, no pre-treatment biopsy material was available. Consequently, the direct effect of neoadjuvant therapy on the tumor immune heterogeneity cannot be interpreted as causal effects and may reflect baseline biological variability or therapy-related tissue remodeling. Fourth, the absence of clinical outcome data limited the ability to relate heterogeneity measures to treatment response or survival. In addition, limited tissue availability and missing data reduced the number of cases, which is an inherent challenge in spatial tissue-based studies. Finally, since the concept design of this study, several new multiplex tissue imaging, spatial transcriptomics and single cell sequencing technologies have become available that allow large-scale analysis of the intratumor immunological landscape (39). However, these technologies are still quite expensive and time and resource consuming which does not allow them to be implemented for wider use in the clinical setting. Future studies incorporating these technologies in larger prospective cohort studies, along with more extensive immunological and molecular characterization, may further strengthen the biological and clinical interpretation of spatial tumor immune heterogeneity.

Conclusions

In conclusion, this exploratory, simulation-based study demonstrated that increasing biopsy core size is associated with a reduction of intratumor heterogeneity across most immune markers, suggesting improved sampling representativeness with larger biopsy core sizes. However, PD-L1$^+$ cells remained spatially heterogeneously distributed even in large biopsies, indicating that single biopsy samples may not reflect its spatial distribution within the tumor.

Overall, these findings highlight the complexity of capturing spatial immune heterogeneity using limited tissue samples. Further validation in larger prospective cohort studies will be essential to determine the translational relevance of heterogeneity metrics and to better inform biopsy sampling strategies in routine clinical practice.

Acknowledgments

None.

Footnote

Reporting Checklist: The authors have completed the

© AME Publishing Company.

STROBE reporting checklist. Available at https://tlcr.amegroups.com/article/view/10.21037/tlcr-2026-1-0017/rc

Data Sharing Statement: Available at https://tlcr.amegroups.com/article/view/10.21037/tlcr-2026-1-0017/dss

Peer Review File: Available at https://tlcr.amegroups.com/article/view/10.21037/tlcr-2026-1-0017/prf

Funding: None.

Conflicts of Interest: All authors have completed the ICMJE uniform disclosure form (available at https://tlcr.amegroups.com/article/view/10.21037/tlcr-2026-1-0017/coif). The authors have no conflicts of interest to declare.

Ethical Statement: The authors are accountable for all aspects of the work in ensuring that questions related to the accuracy or integrity of any part of the work are appropriately investigated and resolved. This study was conducted in accordance with the Declaration of Helsinki and its subsequent amendments. The study was approved by the Medical Ethics Committee of UZ/KU Leuven (S56031). All patients included in the study have provided written informed consent.

Open Access Statement: This is an Open Access article distributed in accordance with the Creative Commons Attribution-NonCommercial-NoDerivs 4.0 International License (CC BY-NC-ND 4.0), which permits the non-commercial replication and distribution of the article with the strict proviso that no changes or edits are made and the original work is properly cited (including links to both the formal publication through the relevant DOI and the license). See: https://creativecommons.org/licenses/by-nc-nd/4.0/.

References

1. Spigel DR, Faivre-Finn C, Gray JE, et al. Five-Year Survival Outcomes From the PACIFIC Trial: Durvalumab After Chemoradiotherapy in Stage III Non-Small-Cell Lung Cancer. J Clin Oncol 2022;40:1301-11.
2. Novello S, Kowalski DM, Luft A, et al. Pembrolizumab Plus Chemotherapy in Squamous Non-Small-Cell Lung Cancer: 5-Year Update of the Phase III KEYNOTE-407 Study. J Clin Oncol 2023;41:1999-2006.
3. Garassino MC, Gadgeel S, Speranza G, et al. Pembrolizumab Plus Pemetrexed and Platinum in Nonsquamous Non-Small-Cell Lung Cancer: 5-Year Outcomes From the Phase 3 KEYNOTE-189 Study. J Clin Oncol 2023;41:1992-8.
4. Girard N, Bar J, Garrido P, et al. Treatment Characteristics and Real-World Progression-Free Survival in Patients With Unresectable Stage III NSCLC Who Received Durvalumab After Chemoradiotherapy: Findings From the PACIFIC-R Study. J Thorac Oncol 2023;18:181-93.
5. Forde PM, Spicer JD, Provencio M, et al. Overall Survival with Neoadjuvant Nivolumab plus Chemotherapy in Lung Cancer. N Engl J Med 2025;393:741-52.
6. Heymach JV, Harpole D, Mitsudomi T, et al. Perioperative Durvalumab for Resectable Non-Small-Cell Lung Cancer. N Engl J Med 2023;389:1672-84.
7. Provencio M, Nadal E, González-Larriba JL, et al. Perioperative Nivolumab and Chemotherapy in Stage III Non-Small-Cell Lung Cancer. N Engl J Med 2023;389:504-13.
8. Wakelee H, Liberman M, Kato T, et al. Perioperative Pembrolizumab for Early-Stage Non-Small-Cell Lung Cancer. N Engl J Med 2023;389:491-503.
9. Signorelli D, Giannatempo P, Grazia G, et al. Patients Selection for Immunotherapy in Solid Tumors: Overcome the Naïve Vision of a Single Biomarker. Biomed Res Int 2019;2019:9056417.
10. Błach J, Wojas-Krawczyk K, Nicoś M, et al. Failure of Immunotherapy-The Molecular and Immunological Origin of Immunotherapy Resistance in Lung Cancer. Int J Mol Sci 2021;22:9030.
11. Sharma P, Hu-Lieskovan S, Wargo JA, et al. Primary, Adaptive, and Acquired Resistance to Cancer Immunotherapy. Cell 2017;168:707-23.
12. Kluger HM, Tawbi HA, Ascierto ML, et al. Defining tumor resistance to PD-1 pathway blockade: recommendations from the first meeting of the SITC Immunotherapy Resistance Taskforce. J Immunother Cancer 2020;8:e000398.
13. Hellmann MD, Rizvi NA, Goldman JW, et al. Nivolumab plus ipilimumab as first-line treatment for advanced non-small-cell lung cancer (CheckMate 012): results of an open-label, phase 1, multicohort study. Lancet Oncol 2017;18:31-41.
14. Johnson ML, Cho BC, Luft A, et al. Durvalumab With or Without Tremelimumab in Combination With

Chemotherapy as First-Line Therapy for Metastatic Non-Small-Cell Lung Cancer: The Phase III POSEIDON Study. J Clin Oncol 2023;41:1213-27.
15. Paz-Ares L, Spira A, Raben D, et al. Outcomes with durvalumab by tumour PD-L1 expression in unresectable, stage III non-small-cell lung cancer in the PACIFIC trial. Ann Oncol 2020;31:798-806.
16. Wu W, Liu Y, Zeng S, et al. Intratumor heterogeneity: the hidden barrier to immunotherapy against MSI tumors from the perspective of IFN-γ signaling and tumor-infiltrating lymphocytes. J Hematol Oncol 2021;14:160.
17. Vitale I, Shema E, Loi S, et al. Intratumoral heterogeneity in cancer progression and response to immunotherapy. Nat Med 2021;27:212-24.
18. Marusyk A, Janiszewska M, Polyak K. Intratumor Heterogeneity: The Rosetta Stone of Therapy Resistance. Cancer Cell 2020;37:471-84.
19. Fridman WH, Pagès F, Sautès-Fridman C, et al. The immune contexture in human tumours: impact on clinical outcome. Nat Rev Cancer 2012;12:298-306.
20. Gerlinger M, Rowan AJ, Horswell S, et al. Intratumor heterogeneity and branched evolution revealed by multiregion sequencing. N Engl J Med 2012;366:883-92.
21. McGranahan N, Swanton C. Clonal Heterogeneity and Tumor Evolution: Past, Present, and the Future. Cell 2017;168:613-28.
22. Seoane J, De Mattos-Arruda L. The challenge of intratumour heterogeneity in precision medicine. J Intern Med 2014;276:41-51.
23. Sharma A, Merritt E, Hu X, et al. Non-Genetic Intra-Tumor Heterogeneity Is a Major Predictor of Phenotypic Heterogeneity and Ongoing Evolutionary Dynamics in Lung Tumors. Cell Rep 2019;29:2164-2174.e5.
24. McLaughlin J, Han G, Schalper KA, et al. Quantitative Assessment of the Heterogeneity of PD-L1 Expression in Non-Small-Cell Lung Cancer. JAMA Oncol 2016;2:46-54.
25. Ilie M, Long-Mira E, Bence C, et al. Comparative study of the PD-L1 status between surgically resected specimens and matched biopsies of NSCLC patients reveal major discordances: a potential issue for anti-PD-L1 therapeutic strategies. Ann Oncol 2016;27:147-53.
26. Sehgal IS, Agarwal R, Dhooria S, et al. Role of EBUS TBNA in Staging of Lung Cancer: A Clinician's Perspective. J Cytol 2019;36:61-4.
27. Sung S, Heymann JJ, Crapanzano JP, et al. Lung cancer cytology and small biopsy specimens: diagnosis, predictive biomarker testing, acquisition, triage, and management. J Am Soc Cytopathol 2020;9:332-45.
28. Jalil BA, Yasufuku K, Khan AM. Uses, limitations, and complications of endobronchial ultrasound. Proc (Bayl Univ Med Cent) 2015;28:325-30.
29. Bankhead P, Loughrey MB, Fernández JA, et al. QuPath: Open source software for digital pathology image analysis. Sci Rep 2017;7:16878.
30. Kashyap A, Rapsomaniki MA, Barros V, et al. Quantification of tumor heterogeneity: from data acquisition to metric generation. Trends Biotechnol 2022;40:647-76.
31. Mei J, Xiao Z, Guo C, et al. Prognostic impact of tumor-associated macrophage infiltration in non-small cell lung cancer: A systemic review and meta-analysis. Oncotarget 2016;7:34217-28.
32. Becherini C, Lancia A, Detti B, et al. Modulation of tumor-associated macrophage activity with radiation therapy: a systematic review. Strahlenther Onkol 2023;199:1173-90.
33. Ben-Mordechai T, Lawrence YR, Symon Z, et al. CX3CR1-Expressing Immune Cells Infiltrate the Tumor Microenvironment and Promote Radiation Resistance in a Mouse Model of Lung Cancer. Cancers (Basel) 2023;15:5472.
34. Munari E, Zamboni G, Lunardi G, et al. PD-L1 Expression Heterogeneity in Non-Small Cell Lung Cancer: Defining Criteria for Harmonization between Biopsy Specimens and Whole Sections. J Thorac Oncol 2018;13:1113-20.
35. Chen M, Xu Y, Zhao J, et al. Feasibility and reliability of evaluate PD-L1 expression determination using small biopsy specimens in non-small cell lung cancer. Thorac Cancer 2021;12:2339-44.
36. Gompelmann D, Sinn K, Brugger J, et al. Correlation of PD-L1 expression on tumour cells between diagnostic biopsies and surgical specimens of lung cancer in real life with respect to biopsy techniques and neoadjuvant treatment. J Cancer Res Clin Oncol 2023;149:1747-54.
37. Sun W, Yang X, Wang H, et al. Among Multiple Needle Core Biopsy Samples, the One with the Highest Tumor Proportion Score Best Represents the PD-L1 Status of the Whole Surgical Specimen in Non-Small Cell Lung Cancer. Appl Immunohistochem Mol Morphol

© AME Publishing Company.

2022;30:190-6.
38. Clark BZ, Onisko A, Assylbekova B, et al. Breast cancer global tumor biomarkers: a quality assurance study of intratumoral heterogeneity. Mod Pathol 2019;32:354-66.
39. Patkar S, Chen A, Basnet A, et al. Predicting the tumor microenvironment composition and immunotherapy response in non-small cell lung cancer from digital histopathology images. NPJ Precis Oncol 2024;8:280.

Cite this article as: Lyu S, Reynders K, Laven IEWG, Faes C, Weynand B, Hillen LM, De Leyn P, Hendriks LEL, Wauters E, Lambrecht M, Vaes RDW, De Ruysscher D. Intratumor immune heterogeneity across simulated core biopsy sizes in non-small cell lung cancer: an exploratory study. Transl Lung Cancer Res 2026;15(7):200. doi: 10.21037/tlcr-2026-1-0017

© AME Publishing Company.